American Mineralogist, Volume 83, pages 300–304, 1998

Full multiple scattering calculations of the X-ray absorption near edge structure at the magnesium K-edge in pyroxene

DELPHINE CABARET,[1] PHILIPPE SAINCTAVIT,[1,2] PHILIPPE ILDEFONSE,[1] AND ANNE-MARIE FLANK[2]

[1]Laboratoire de Minéralogie-Cristallographie, CNRS URA 9, Universités Paris 6 et 7, 4 place Jussieu, 75252 Paris Cedex 05, France
[2]Laboratoire de l'Utilisation du Rayonnement Electromagnétique, Bât. 209d, Université Paris-Sud, 91405 Orsay, France

ABSTRACT

We present a comparison between XANES experiments and full multiple-scattering calculations at the magnesium K-edge for two pyroxenes, diopside and enstatite, for which Mg atoms are only in the M1 site and in two distinct sites M1 and M2, respectively. The influence of the number of octahedral sites per unit cell and of the site distortion on Mg K-edge XANES spectra is investigated. Good agreement between experiment and calculations is obtained. Full multiple-scattering calculations permit identification of the contribution of each site. Comparison reveals that the Mg K-edge spectra of enstatite and diopside M1 sites have the same XANES profile. Cluster size analysis shows that most Mg K-edge XANES features are related to medium range order, i.e., 6 Å around the absorbing atom. We therefore clearly define the Mg K-edge signature of the geometrical arrangement of atoms around each site, M1 and M2.

INTRODUCTION

Pyroxenes are an important group of rock-forming ferromagnesian silicates. They are widespread in crustal and upper mantle rocks of basaltic and ultramafic compositions and occur as stable phases in almost every type of igneous rock. Pyroxenes have been extensively studied in mineralogy and petrology. Understanding the crystallographic, chemical, and physical properties is still of great interest in earth and environmental sciences (Yang and Ghose 1995; Wentzcovitch et al. 1995; Dimanov et al. 1996).

X-ray absorption spectroscopy is a powerful technique for structural characterization of minerals. Notably, X-ray absorption in the vicinity of absorption edges (commonly called XANES: X-ray Absorption Near Edge Structure) is highly sensitive to the geometrical environment around the absorbing atom and its medium range organization. Full multiple scattering (FMS) calculations allow interpretation of X-ray absorption spectra even in structurally complex materials (Wu et al. 1996a, 1996b, 1996c; Cabaret et al. 1996). We used this method to interpret Al K-edge spectra in oxides and silicates with various coordination numbers (Cabaret et al. 1996). Most XANES studies related to pyroxenes involve the energy range 4 keV-8 keV: Paris and Tyson (1994) interpreted Fe K-edge XANES spectra of the orthoferrosilite $Fe_2Si_2O_6$ by FMS theory and compared the results with wüstite (FeO). Farges (1995) also examined the Fe-K edge in orthopyroxene (Fe-bearing $Mg_2Si_2O_6$) to investigate the iron substitution processes. Paris et al. (1995) characterized the calcium environment in omphacitic pyroxenes, comparing Ca K-edge XANES spectra with FMS calculations. More recently, Closmann et al. (1996) presented an experimental and theoretical EXAFS study of the crystal chemistry of $(Mg_{0.88}Fe_{0.12})SiO_3$ at the Fe K-edge.

In contrast, Mg K-edge XANES spectra in pyroxenes have not been widely studied because measurements in the energy range 1000–2000 eV proved to be difficult (Mottana et al. 1996). Furthermore, the theoretical interpretation of XANES in complex materials is a delicate matter. In the literature, most Mg K-edge studies are related to MgO. This compound is used as a reference due to its cubic structure, and is also an important substrate for numerous studies in surface physics (Wu et al. 1996b; Aritani et al. 1996; Yoshida et al. 1995; Tanaka et al. 1995). Experimental studies of Mg K edge XANES in minerals have been the subject of two papers: Ildefonse et al. (1995) present Mg K-edge spectra of crystalline model compounds such as spinel, periclase, pyrope, and diopside; and Mottana et al. (1996) briefly compare experimental data with calculations at the Mg K-edge of diopside and omphacite. To our knowledge, no detailed multiple-scattering analysis at the Mg K-edge in pyroxenes has been carried out. In this paper, we present FMS calculations at the magnesium K-edge in two pyroxenes that we compare with experiments: Enstatite, which is characterized by two different sites for Mg atoms, and the clinopyroxene diopside, in which Mg atoms only occupy one type of site. Thus, our purpose is to clearly determine how the number of octahedral sites on the one hand and the site distortion on the other hand affect the Mg K-edge XANES spectra.

EXPERIMENTAL AND THEORETICAL METHODS

Diopside and enstatite samples from Kilbourne Hole ultramafic xenoliths, New Mexico, have the following compositions: diopside = $(Na_{0.08}Ca_{0.78}Mg_{0.14})(Mg_{0.78}Fe_{0.08}$

0003–004X/98/0304–0300$05.00

$Cr_{0.04}Al_{0.10})(Si_{1.89}Ti_{0.01}Al_{0.10})_{06}$; enstatite = $(Na_{0.01}Ca_{0.04}Mg_{0.93})(Mg_{0.76}Fe_{0.15}Cr_{0.02}Al_{10.07})(Si_{1.94}A_{0.06})_{06}$ (Glücklich-Herbas 1992). Mg K-edge spectra were recorded on the SA32 beam line of the French storage ring Super-ACO using a two-barrel monochromator. The super-ACO ring was operating at 800 MeV (λ_c = 18.6 Å) with a beam current in the range 100–300 mA. Powder samples are directly mounted on copper slides after dispersion in acetone. The sample holder was transferred into the sample chamber where the pressure is below 1 mPa. Mg K-edge spectra were collected at room temperature over a photon energy range of 1300–1380 eV in 0.2 eV steps. The data were collected using entrance slits giving an energy resolution of about 0.5 eV. Energy calibration was made using the Cu L_3-edge absorption peak of CuO (931.2 eV, Cartier et al. 1990). Total electron yield detection was carried out by recording the total drain current for I and I_0.

X-ray absorption spectra were calculated in the FMS formalism, with the "extended Continuum" code developed by Natoli et al. (1980). The absorbing atom and surrounding atoms are modeled by a monoelectronic "muffin-tin" potential. The potential was constructed following the approach described by Levelut et al. (1995). Convergence of the basis functions for the final state were tested by calculating the total cross section for several values of l_{max}, the maximum orbital angular momentum, in the range $3 \leq l_{max} \leq 5$. For all calculations the angular wave function expansion could be truncated at $l_{max} = 3$. The best results were obtained with the "relaxed and screened" potential calculated in the "Z + 1" approximation for the excited state and with a real Dirac-Hara exchange potential (Cabaret et al. 1996). An overlap factor of 10% was used for the atomic sphere radii and chosen using the Norman prescriptions (Norman 1976). Overlapping spheres have the advantage of reducing the volume of the interstitial region, where the approximation to the potential is the poorest (Kutzler et al. 1980). Initially, calculations were performed for large clusters, about 8 Å in radius. Then the cluster size was decreased to examine the influence of medium range order on the features in the XANES spectra. The calculated spectra were convolved with a Lorentzian function whose width at half maximum is related to the effective mean free path of the photoelectron, which takes into account the instrumental resolution (0.5 eV), the finite lifetime of the core hole (0.36 eV, Krause and Oliver 1979), and the inelastic scattering of the photoelectron by the electrons in the materials. Because the "Continuum" code yield only energies relative to the muffin-tin zero, the theoretical and the experimental spectra have been aligned at the maximum of the first strong resonance (labeled A).

Full multiple scattering calculations

Diopside

Diopside crystallizes in the monoclinic system with a = 9.75, b = 8.90, c = 5.25 Å, and β = 105.63°. The unit cell contains four $CaMgSi_2O_6$ units and the space group is $C2/c$. Mg atoms are in M1 sites, which have sixfold coordination with respect to O atoms in fairly regular octahedra. Ca atoms are located in irregular eightfold-coordinated sites, labeled M2. For details, see Cameron et al. (1972) or Smyth and Bish (1988).

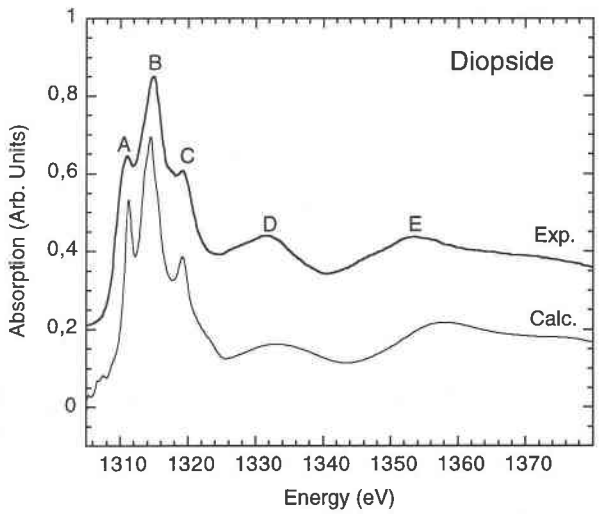

FIGURE 1. Experimental and calculated Mg K-edge spectra of diopside.

Experimental and calculated Mg K-edge X-ray absorption spectra of diopside are displayed in Figure 1. The experimental spectrum is characterized by three well-resolved peaks near the edge (A at 1310.4, B at 1314.4, and C at 1318.8 eV), and two broader resonances D and E at around 1331.8 and 1354.7 eV, respectively. The calculations were performed with a cluster of radius 8 Å. It is clear that all the experimental features are well reproduced by the FMS calculations.

To determine the volume seen by the photoelectron, we performed a cluster size analysis. Figure 2 shows spectra calculated for various cluster sizes, starting from a 7-atom cluster, i.e., the absorbing atom and its coordination shell, up to an 8.0 Å radius. Cluster compositions are reported in Table 1. Features A, B, and C are well resolved only for large clusters (more than 7 Å in radius). Although the 7.3 and 8.0 Å radius clusters reproduce these peaks, the agreement with experiment, in terms of relative intensities, is better for the 8.0 Å radius cluster. Therefore peaks A, B, and C are clearly related to medium range order. Feature E is present in the coordination shell spectrum and is therefore a signature of the local atomic arrangement around the absorbing atom. It can be mainly assigned to multiple scattering in the coordination sphere.

Enstatite

Enstatite is orthorhombic with a = 18.23 Å, b = 8.82 Å, c = 5.18 Å. The unit cell contains eight $Mg_2Si_2O_6$ units (space group $Pbca$). In contrast to diopside, Mg atoms are in two distinct sites, M1 and M2, with point symmetry 1. M1 is still a fairly regular octahedron, as it was

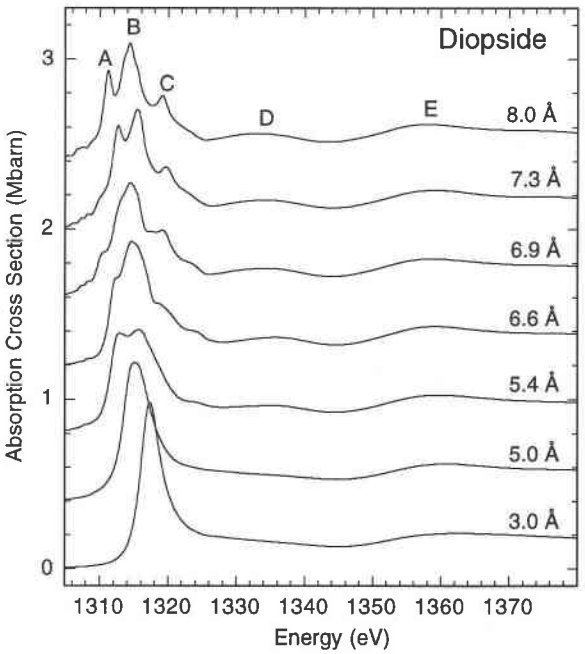

FIGURE 2. FMS calculations of diopside for various cluster radii, indicated above each curve (in angstroms).

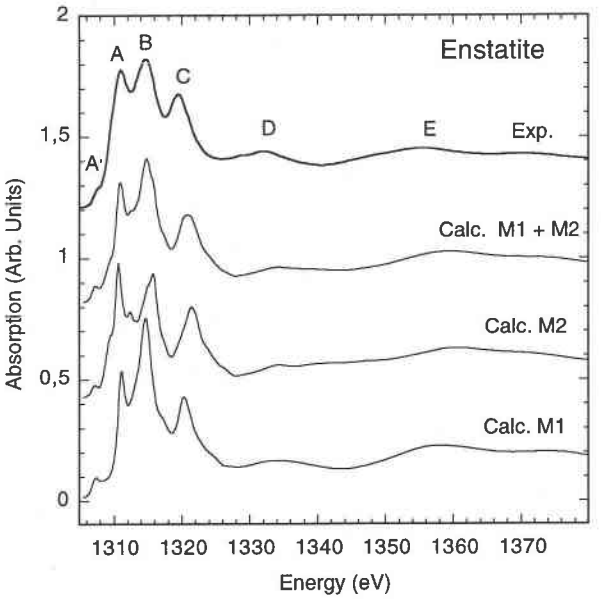

FIGURE 3. Mg K-edge spectra of enstatite. The spectra, from top to the bottom, respectively, are the experimental spectrum, the calculated spectrum with contributions from Mg in both M1 and M2 sites, the calculated spectrum from M1 site only, and the calculated spectrum from M2 site only.

the case for diopside, whereas M2 is a strongly distorted sixfold-coordinated site (Yang and Ghose 1982). For details see Sasaki et al. (1982) and Smyth and Bish (1988).

Calculations and experiment are compared in Figure 3. Because two sites exist for Mg atoms in the enstatite structure, the experimental spectrum (with weak peak A′, three main resonances A, B, and C located respectively at 1310.8, 1314.4, and 1319.4 eV and two broad features D and E, at around 1332 and 1356 eV, respectively) is the sum of two contributions corresponding to the absorbing atom in each site. To evaluate the effects of site geometry and discriminate between the contributions for each site, FMS calculations have been carried out twice, by locating the absorbing atom either in M1 (noted Calc. M1) or in M2 (Calc. M2) and then summing (Calc. M1 + M2). These calculations were performed with 7.6 Å radius clusters. We obtain a fairly good agreement between experiment and the summed M1 and M2 contributions. All the spectral features are reproduced by the calculation. From the individual M1 and M2 spectra, the intensities of the features can be compared to assign the origin of the resonances present in the Calculation M1 + M2 spectrum. Feature B is more intense in Calculation M1 than in Calculation M2. Therefore the contribution to B, originating from Mg in M1 site, is more important than that originating from Mg in M2 site. On the other hand, the contributions to features A, C, D, and E almost equally come from both sites, although D and E peaks are broader in the Calculation M2 spectrum than in the Calculation M1.

Calculations performed with various cluster sizes (Table 1) for the absorbing atom in M1 and M2 sites are plotted in Figure 4. For Ml, the main resonances (A, B, and C) are well defined only for the largest clusters: the 7.1 and the 7.6 Å radius clusters. Feature C appears as a shoulder in the 4.4 Å radius spectrum and tends to be-

TABLE 1. Cluster compositions

Diopside					Enstatite M1				Enstatite M2			
Radius (Å)	Composition				Radius (Å)	Composition			Radius (Å)	Composition		
3.0	1 Mg	6 O			3.0	1 Mg	6 O		3.3	1 Mg	6 O	
5.0	3 Mg	8 O	6 Si	3 Ca	4.4	6 Mg	9 O	6 Si	4.4	4 Mg	9 O	5 Si
5.4	3 Mg	20 O	8 Si	3 Ca	5.3	6 Mg	22 O	7 Si	5.3	4 Mg	22 O	8 Si
6.6	5 Mg	34 O	8 Si	5 Ca	6.1	10 Mg	38 O	11 Si	6.0	9 Mg	37 O	10 Si
6.9	7 Mg	42 O	20 Si	8 Ca	6.6	13 Mg	39 O	17 Si	6.6	18 Mg	44 O	16 Si
7.3	7 Mg	60 O	20 Si	12 Ca	7.1	20 Mg	56 O	20 Si	7.2	23 Mg	53 O	17 Si
8.0	13 Mg	90 O	30 Si	14 Ca	7.6	26 Mg	79 O	25 Si	7.6	28 Mg	75 O	22 Si

come more intense and narrower with increasing cluster size. Resonance D clearly appears in the spectrum calculated with a 5.3 Å radius cluster and is well resolved for the 6.1 Å spectrum. As in diopside, the 3.0 Å radius cluster calculation exhibits feature E, from which we deduce that E is mainly due to the first coordination shell. For M2, spectra calculated with cluster radius larger than 6.0 Å display the three well-defined A, B, and C features. Feature B appears in the 4.4 Å radius cluster calculation and becomes well resolved in a cluster with a radius of 7.2 Å. Adding more atomic shell does not yield significant changes in the shape and the intensity of this peak. Figure 3 shows that experimental feature C contains equal contributions from Mg in M1 and M2 sites. This cluster size analysis gives the following additional information: Feature C is due to multiple scattering effects inside a sphere of radius of about 6 Å around the M2 site and inside a sphere of radius of about 7.6 Å around the M1 site. The lowermost curves of Figures 4a and 4b, which represent the influence of the coordination sphere on the spectra, both exhibit one main peak around 1316 eV, which is more intense and narrower in the M1 spectrum than in the M2 spectrum. These differences can be related to the fact that the M2 Mg site is more distorted than the M1 site. This point is further discussed in the next section.

Discussion

The Mg-K edge XANES spectra of enstatite and diopside up to 1545 eV are dominated by medium range order, because only calculations performed with cluster radii greater than 6 Å reproduce most of the XANES features. This result has already been observed at K-edge of low Z-elements in mineralogical compounds: at the magnesium K-edge (Wu et al. 1996b), at the aluminum K-edge (Wu et al. 1996b, 1997; Cabaret et al. 1996), and at the silicon K-edge (Wu et al. 1996c; Wu and Seifert 1996). It relates to the large mean free path of the photoelectron near the edge. Calculation of the imaginary part of the photoelectron self-energy, suggests that the mean free path could reach 40 Å near the edge.

Although calculations with large clusters are essential to mimic the spectra, coordination shell calculations can provide information about the distortion of the site of the absorbing atom (Paris and Tyson 1994; Cabaret et al. 1996). Calculations with a coordination sphere cluster (7 atoms) for M1 sites in diopside and enstatite (Figs. 2 and 4a) show an intense and narrow resonance. The same coordination sphere cluster calculation for M2 site in enstatite (Fig. 4b) shows a broad resonance with some structure. The difference between M1 and M2 calculations can be directly related to the fact that M1 sites resemble a regular octahedron whereas M2 sites are strongly distorted. M1 sites in both structures are similar, although the exact symmetry point group is 2 for diopside whereas it is 1 for enstatite. An evaluation of the geometry of octahedral sites can be expressed in terms of quadratic elongation (QE) and angular variance (AV) (Robinson et al. 1971). From Cameron et al. (1972), Sasaki et al. (1982), and Smith and Bish (1988), QE is equal to 1.0050 and 1.0088 and AV is equal to 17.4 and 26.5 for the M1 sites in diopside and enstatite, respectively. These values are close to each other in contrast to those of enstatite M2 site, which are very distorted: QE = 1.0489 and AV = 140. Furthermore, the Mg–O mean distances of both M1 sites are identical and equal to 2.08 Å, while that of enstatite M2 site is 2.15 Å (e.g., Smith and Bish 1988). Although the average bond length, the quadratic elongation, and the angle variance are useful numbers to discriminate between different types of sites, the average angle does not provide much information.

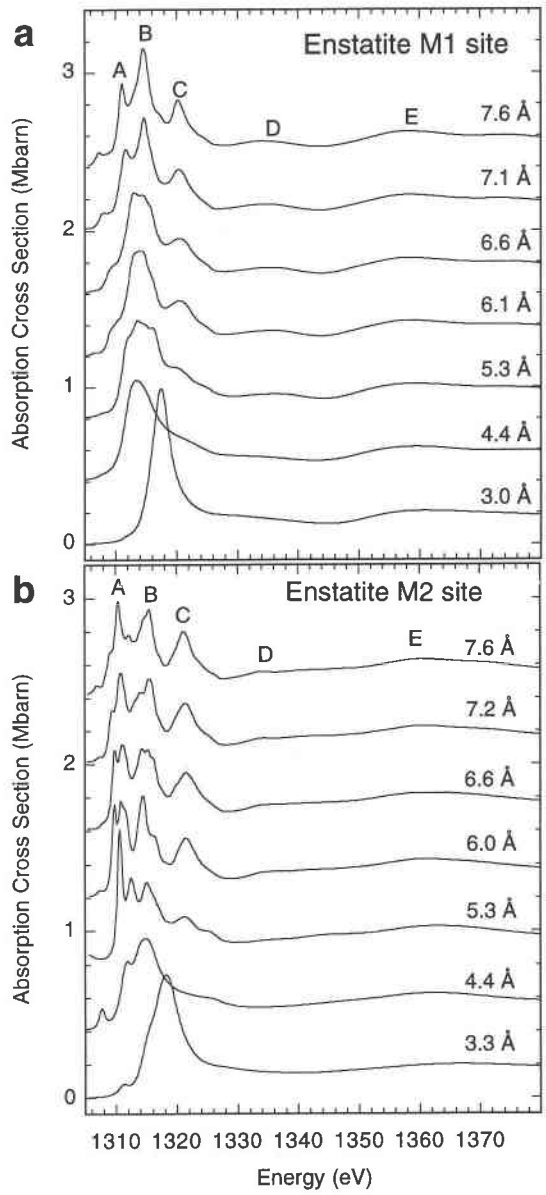

Figure 4. FMS calculations of enstatite for various cluster radii (in angstroms). (**a**) M1 site. (**b**) M2 site.

The theoretical spectrum of the enstatite M1 site (Fig. 3) is also virtually identical to that of diopside (Fig. 1). Furthermore, the calculated M1 spectrum of enstatite (Fig. 4a) follows almost the same evolution with cluster size as the calculated diopside spectrum (Fig. 2). Consequently, we assume, with great confidence, that the contribution of M1 site to the enstatite experimental spectrum should look like the diopside experimental spectrum. This assumption has been confirmed by the fact that the spectrum obtained by substracting diopside and enstatite experimental spectra is in good agreement with the calculated M2 site contribution, not only in terms of positions but also in intensities of the resonances. Because M2 sites are occupied by Ca atoms in diopside and Mg atoms in enstatite, we conclude from the preceding discussion that the nature of the atom that occupies the M2 site has a minor influence on the M1 calculated X-ray absorption spectrum.

Both experimental spectra of diopside and enstatite exhibit three main resonances near the edge. The main difference between the two spectra is in the relative intensities of features A and B. The FMS calculations allow the assignment of these differences of intensity to the presence of Mg atom in the M2 site and not to a modification of the local environment around the M1 site due to the substitution of Ca for Mg in the M2 site.

Acknowledgments

This work was partly supported by the EU Human Capital and Mobility network n°ERBCHXCT930360. We are indebted to J. Girardeau for providing natural samples. We are grateful to C. Brouder and F. Cesbron for enlightening conversations, to V. Briois for making part of the calculations possible, and to A. Ramos, E. Balan, and S. Rabii for their thorough reading of the manuscript. This is the IPGP contribution no. 1494.

References cited

Aritani, H., Tanaka, T., Funabiki, T., Yoshida, S., Kudo, M., and Hasegawa, S. (1996) Structure of Mo-Mg binary oxides in oxidized/reduced states studied by x-ray absorption spectroscopy at the Mo K edge and Mg K edge. Journal of Physical Chemistry, 100, 5440–5446.

Cabaret, D., Sainctavit, P., Ildefonse, P., and Flank, A.-M. (1996) Full multiple-scattering calculations on silicates and oxides at the Al K edge. Journal of Physics: Condensed Matter, 8, 3691–3704.

Cameron, M., Sueno, S., Prewitt, C.T., and Papike, J.J. (1973) High temperature crystal chemistry of acmite, diopside, hedenbergite, jadeite, spodumene, and uyerite. American Mineralogist, 58, 594–618.

Cartier, C., Verdaguer, M., Flank, A.-M., Lagarde, P., Baudelet, F., Darriet, J., Tressaud, A., and Lelirzin, A. (1990) K and $L_{2,3}$ absorption edges of copper complexes. In A. Balerna, E. Bernieri, and S. Mobilio, Eds., Proceedings of the 2nd European Conference on Progress in X-Ray Synchrotron Radiation Research, 1041 p. Editrice Compositori, Bologna, Italia.

Closmann, C., Knittle, E., and Bridges, F. (1996) An EXAFS study of the crystal chemistry of Fe in orthopyroxene. American Mineralogist, 81, 1321–1331.

Dimanov, A., Jaoul, O., and Sautter, V. (1996) Calcium self-diffusion in natural diopside single crystals. Geochimica Cosmochimica Acta, 60, 4095–4106.

Farges, F. (1995) The site of Fe in Fe-bearing $MgSiO_3$ enstatite and perovskite. A theoretical-, x-ray multiple-scattering study at Fe K-edge. Physics and Chemistry of Minerals, 22, 318–322.

Glücklich-Herbas, M. (1992) Caractérisation pétrochimique du manteau lherzolitique sous-continental, Ph.D. dissertation, Université Paris 7.

Ildefonse, P., Calas, G., Flank, A.-M., and Lagarde, P. (1995) Low Z elements (Mg, Al, and Si) K-edge x-ray absorption spectroscopy in minerals and disordered systems. Nuclear Instruments and Methods in Physics Research B, 97, 172–175.

Krause, M.O. and Oliver, J.H. (1979) Natural widths of atomic K and L levels, Kα X-ray lines and several KLL Auger lines. Journal of Physical and Chemical Reference Data, 8, 329–338.

Kutzler, F.W., Natoli, C.R., Misemer, D.K., Doniach, S., and Hodgson, K.O. (1980) Use of the one-electron theory for the interpretation of the near edge structure in K-shell x-ray absorption spectra of transition metal complexes. The Journal of Chemical Physics, 73, 3274–3288.

Levelut, C., Sainctavit, P., Ramos, A., and Petiau, J. (1995) Linear x-ray dichroism of cadmium sulphide with wurtzite and zincblende structure. Journal of Physics: Condensed Matter, 7, 2353–2367.

Mottana, A., Murata, T., Wu, Z., Marcelli, A., and Paris, E. (1996) Detection of order-disorder in pyroxenes of the jadeite-diopside series via XAS at the Ca-Na and Mg-Al K-edges. Journal of Electron Spectroscopy and Related Phenomena, 79, 79–82.

Natoli, C.R., Misemer, D.K., and Doniach, S. (1980) First-principles calculation of x-ray absorption- edge structure in molecular clusters. Physical Review A, 22, 1104–1108.

Norman, J.G., Jr. (1976) Non-empirical versus experimental choices for overlapping sphere radii ratios in SCF-Xα-SW calculations on ClO_4^- and SO_2. Molecular Physics, 31, 1191–1198.

Paris, E. and Tyson, T.A. (1994) Iron site geometry in orthopyroxene: multiple scattering calculations and XANES study. Physics and Chemistry of Minerals, 21, 299–308.

Paris, E., Wu, Z., Mottana, A., and Marcelli, A. (1995) Calcium environment in omphacitic pyroxenes: XANES experimental data versus one-electron multiple scattering calculations. European Journal of Mineralogy, 7, 1065–1070.

Robinson, K., Gibbs, G.V., and Ribbe, P.H. (1971) Quadratic elongation: a quantitative measure of distortion in coordination polyhedra. Science, 172, 576–570.

Sasaki, S., Takeuchi, Y., Fujino, K., and Akimoto, S.-I. (1982) Electron-density distributions of three orthopyroxenes, $Mg_2Si_2O_6$, $Co_2Si_2O_6$, and $Fe_2Si_2O_6$. Zeitschrift für Kristallographie, 158, 279–297.

Smyth, J.R. and Bish, D.L. (1988) Crystal Structures and Cation Sites of Rock-Forming Minerals, 332 p. Allen and Unwin, Boston.

Tanaka, I., Kawai, J., and Adachi, H. (1995) Calculation of electron energy-loss near edge structures using a model cluster of MgO. Solid State Communications, 93, 533–536.

Wentzcovitch, R.M., Hugh-Jones, D.A., Angel, R.J., and Price, G.D. (1995) Ab initio study of $MgSiO_3$ C2/c enstatite. Physics and Chemistry of Minerals, 22, 453–460.

Wu, Z. and Seifert, F. (1996) Theoretical analysis of Si and O XANES spectra of zircon vs α-quartz. Solid State Communications, 99, 773–778.

Wu, Z., Marcelli, A., Mottana, A., Giuli, G., Paris, E., and Seifert, F. (1996a) Effects of higher shells in garnets detected by x-ray absorption spectroscopy at the Al K-edge. Physical Review B, 54, 2976–2979.

Wu, Z., Mottana, A., Marcelli, A., Natoli, C.R., and Paris, E. (1996b) Theoretical analysis of x-ray absorption near-edge structure in forsterite, Mg_2SiO_4-*Pbnm,* and fayalite, Fe_2SiO_4-*Pbnm,* at room temperature and extreme condition. Physics and Chemistry of Minerals, 23, 193–204.

Wu, Z., Seifert, F., Poe, B., and Sharp, T. (1996c) Multiple-scattering calculations for SiO_2 polymorphs: a comparison to ELNES and XANES spectra. Journal of Physics: Condensed Matter, 8, 3323–3336.

Wu, Z., Marcelli, A., Mottana, A., Giuli, G., and Paris, E. (1997) Al coordination and local structure in minerals: XAFS determinations and multiple-scattering calculations for K-feldspars. Europhysics Letters, 38, 465–470.

Yang, H. and Ghose, S. (1995) High temperature single crystal x-ray diffraction studies of the ortho-proto phase transition in enstatite, $Mg_2Si_2O_6$ at 1360 K. Physics and Chemistry of Minerals, 22, 300–310.

Yoshida, T., Tanaka, T., Yoshida, H., Funabiki, T., Yoshida, S., and Murata, T. (1995) Study of dehydration of magnesium hydroxide. Journal of Physical Chemistry, 99, 10890–10896.

Manuscript received July 21, 1997
Manuscript accepted November 4, 1997